Transport and Relaxation Study of Ionic Phosphate Glasses

Bury Peter[1, a], Hockicko Peter[1,b] and Jamnický Miroslav[2,c]

[1]Department of Physics, Žilina University, 010 26 Žilina, Slovakia

[2]Department of Ceramic, Glass and Cement, Slovak Technical University, 812 37 Bratislava, Slovakia

[a]bury@fel.uniza.sk, [b]hockicko@fyzika.uniza.sk, [c]miroslav.jamnicky@stuba.sk

Keywords: phosphate glasses, acoustic spectroscopy, conductivity and dielectric spectroscopy

Abstract Dynamic processes in glassy materials with ionic conductivity are extremely important since the ion transport significantly affects their practical performance. Conductivity measurement and dielectric relaxation spectroscopy are powerful techniques that reflect the essential features of the transport and relaxational dynamics of the mobile ions that encounter different kinds of site and ionic hopping motion connected with charge mobility. Acoustic spectroscopy is another technique for the study of relaxations in glasses. In this contribution the acoustic and electrical relaxation processes are compared on identical ionic phosphate glasses of the systems $CuI-CuBr-Cu_2O-P_2O_5$ and $CuI-CuBr-Cu_2O-P_2O_5-MoO_3$ containing Cu^+ ions. The acoustic attenuation spectra indicate various relaxation processes and at least two conductivity regimes of transport mechanisms were observed. Both the acoustic and electrical measured data were analyzed using suitable model representations.

Introduction

Characterization of dynamic processes in glassy materials with ionic conductivity is very important since the ion transport significantly affects their practical performance. Conductivity spectroscopy and dielectric relaxation spectroscopy are powerful techniques that reflect the basic features of the relaxation and transport dynamics of the mobile ions [1-3]. Acoustic attenuation spectroscopy is another technique for the study of sub-T_g relaxations in glasses due to a strong acousto-ionic interaction [4, 5]. Relaxation processes occurring on different time scales can be detected in one experiment since the corresponding acoustic loss peaks are spread out on the temperature scale.

Phosphate glasses containing Cu^+ conducting ions have gained attention during last few decades because of their promising potential use in various technological applications. In recent years, several systems of modified phosphate glasses with different cuprous halides and various compositions of glass forming systems were prepared and investigated using IR, SEM, X-ray spectroscopies and some dc conductivity measurements [6-8]. The presence of several structural units, from discrete monomeric to those with three-dimensional networks, were observed.

In this contribution the both acoustic and electrical relaxation processes are transport mechanisms investigated more completely on identical ionic phosphate glasses of the two systems $CuI-CuBr-Cu_2O-P_2O_5$ and $CuI-CuBr-Cu_2O-P_2O_5-MoO_3$ containing Cu^+ ions. Several distinctive peaks in the acoustic attenuation spectra and at least two conductivity regimes of transport mechanisms were observed. The measured data are then analyzed using suitable model representations, discussed and compared.

Experimental

The procedure of glass preparation of both system (18.18–x) CuI – x $CuBr$ – 54.55 Cu_2O – 27.27 P_2O_5 (System I) and system (25.00–y) CuI – y $CuBr$ – 46.875 Cu_2O – 9.375 P_2O_5 – 18.750 MoO_3 (System II) and their complete sets (see Tab. 1) have been already described [6, 7, 9]. However, for

the acoustical attenuation measurements only three samples of System II could be chosen because of their suitable thickness.

The acoustic attenuation measurements using longitudinal acoustic waves of frequency 13, 18 and 27 MHz generated by quartz transducers as well as dc and ac electrical conductivity measurements (50 Hz – 1 MHz) were carried out in the temperature range 140 - 380 K [9, 10]. The quartz buffer was used to separate the acoustic signal from quite short sample. The acoustic attenuation was measured using MATEC attenuation comparator and electrical conductivity was measured using FLUKE impedance analyzer. Guard ring gold electrode configuration including blocking electrode were evaporated on glass discs of the thickness $\approx$ 2 mm and area $\approx$ 1 cm^2 for electrical investigation.

Results and Discussion

The temperature dependencies of dc conductivity for all samples indicate several different transport mechanisms represented with activation energies $E_{a1}{}^{dc}$ - $E_{a4}{}^{dc}$ for first system and $E_{a1}{}^{dc}$ - $E_{a2}{}^{dc}$ for second system. However energies $E_{a3}{}^{dc}$ - $E_{a4}{}^{dc}$ represents probably some dissociation and association processes connected with defect formation [9, 11], that is supported also by repeated measurements, the characteristic feature of which was vanishing of these processes with increasing number of temperature cycles. Besides the activation energies $E_{a2}{}^{d}$ of the system II are practically constant over a wide range of glass composition of CuI/CuBr halides, the activation energies $E_{a1}{}^{dc}$ of this system include a strong mixed cation effect. The representative result of measured dc conductivity (sample BIDP5 and IBPM2) as a function of temperature is illustrated in Fig. 1a. The frequency dependences of ac conductivity measured at various temperatures and frequencies (conductivity spectra) corresponded to the complete conductivity spectra of glassy samples consisting of low frequency plateau regime and dispersive frequency dependent regime [1, 12]. However, an additional deviation of conductivity from the flat ac plateau was observed at low frequencies and higher temperatures obviously referred to electrode polarization [8]. But our measurements indicate more possible transport mechanisms, so that the shift of ac conductivity can represent different hopping centers. The dc conductivity spectra can be fitted then by the equation

$$\sigma(\omega) = \sigma(0) + A\omega^s, \; \sigma(0) = \sigma_0 \exp (E_a{}^{dc}/k_BT) \tag{1}$$

where σ_0 is the pre-exponential factor, $E_a{}^{dc}$ is the activation energies of the ions transport and hopping processes determined from dc measurements. Because the pre-exponential factor σ_0 is function of temperature, the factor σT was used in Arrhenius plots of dc conductivity. The corresponding activation energies $E_{a1}{}^{dc}$ - $E_{a4}{}^{dc}$ are summarized in Table 1.

The imaginary and real part of the complex permittivity $\varepsilon^* (\omega) = \varepsilon'(\omega) - i\varepsilon''(\omega)$ defines the so-called *loss tangent* of the material

$$\tan \delta(\omega) = \varepsilon''(\omega) / \varepsilon'(\omega), \tag{2}$$

that is related to the attenuation constant (or absorption coefficient) of an electromagnetic wave propagating in the material, where $\varepsilon'(\omega)$ and $\varepsilon''(\omega)$ are the real and imaginary parts of the complex permittivity which characterize the *refractive* and *absorptive* properties of the material, respectively. The real and imaginary parts of the complex permittivity were calculated using the sample dimensions and the measured dates of impedance analyzer. The activation energies of the relaxation processes were estimated using the isochronal peaks of tan $\delta(\omega,T)$ from the plots of log f vs. $1/T_{max}$. These plots are straight lines in accordance with Arrhenius equation

$$f = f_0 \exp (E_a{}^{tg\delta}/ k_BT_{max}) , \tag{3}$$

where f is the frequency of applied electrical field, f_0 is the pre-exponential factor and $E_a^{tg\delta}$ is the value of activation energy of the dielectric losses connected with the ion hopping process. The temperature dependences of the loss tangent illustrated in Fig. 2b shows at given frequency range only one broad peak with maximum position (tan δ (T_{max})) shifted to higher temperatures with increasing frequency. But at lower frequencies also another peak can be recognized.
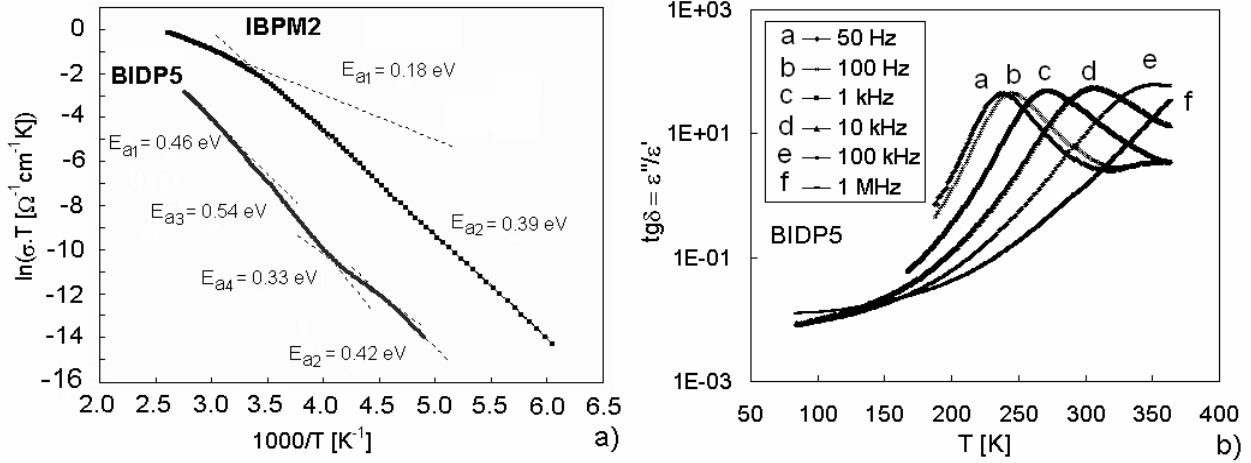

Fig. 1. Representative dc electrical results obtained on BIDP5 (x = 9.09) and IBPM2 (y = 3.125) samples including Arrhenius plot of dc conductivity and temperature dependence of dielectric loss tangent (b) for sample BIDP5.
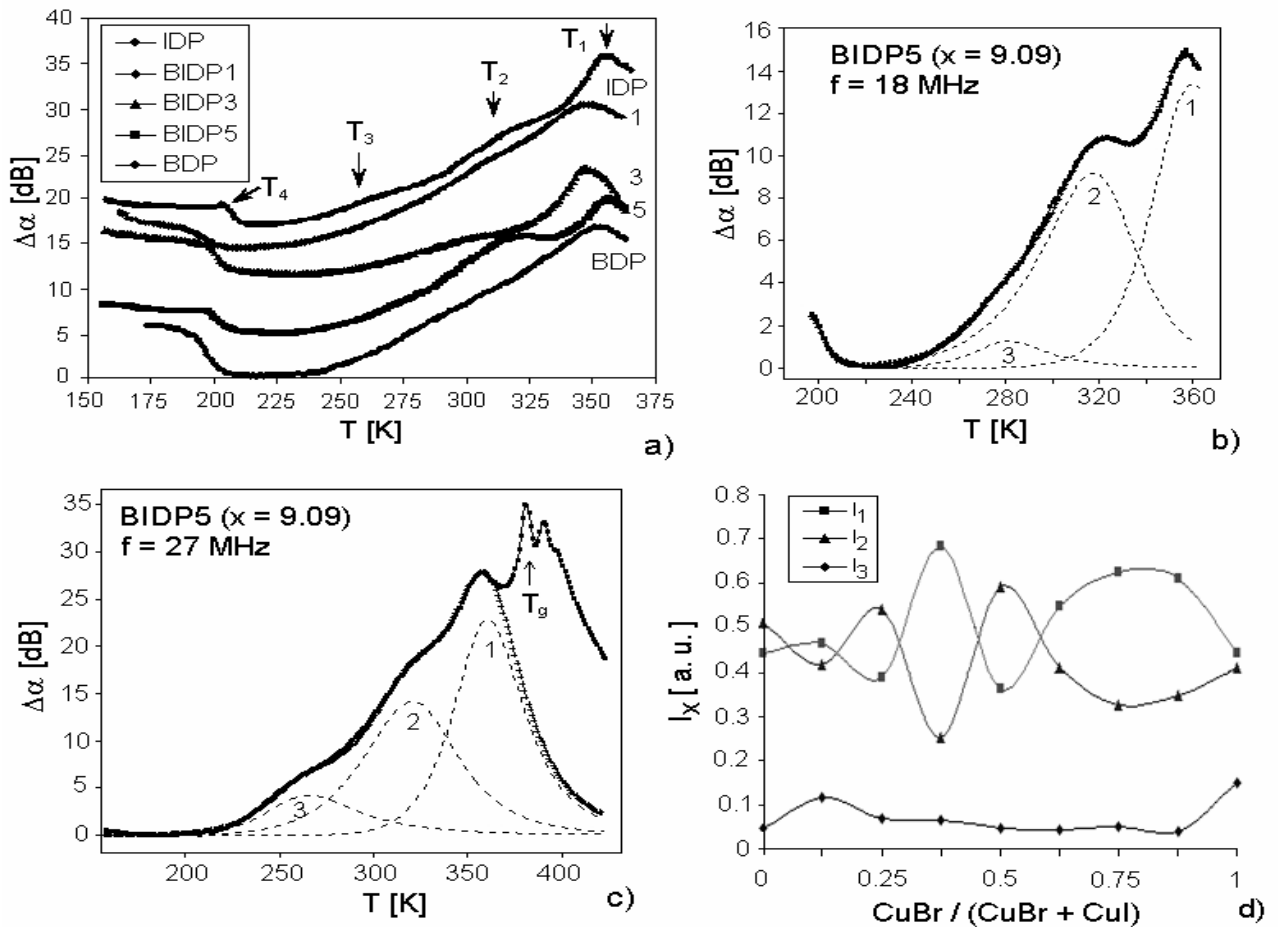

Fig. 2. Acoustics attenuation spectra of several glasses of the System I (a), representative acoustic spectra of sample BIDP5 measured at 18 MHz (b) and 27 MHz (c) and the dependence of the relative peak intensities on glass composition (d). Cross-marked lines represent the best fit as superposition of individual peaks (dashed lines).

The acoustic attenuation spectra of samples of investigated set at all frequencies indicate one broad attenuation peak at higher temperature in which we can distinguish easily two separated peaks (Fig. 2a, 2b).

The acoustic attenuation exhibits a maximum when the relaxation time τ is comparable to the period of the acoustic perturbation ($\omega\tau = 1$), where ω is the angular frequency. The relaxation processes are characterized by activation energy E_a^a for jumps over the barrier between potential minima and typical relaxation frequency of ion hopping $1/\tau_0$. Using the Arrhenius type equation between the peak temperature T_{peak} and the applied frequency ν [5]

$$\nu = \nu_0 \exp\left(-E_a^a/k_B T_{peak}\right) \tag{4}$$

we can determine the value of activation energy of the ion hopping process. Here ν_0 is the pre-exponential factor and k_B is the Boltzmann constant.

The acoustic attenuation spectra of the investigated cuprous halide glasses were gradually fitted using various theoretical attenuation functions including the Debye, Kohlrausch-Williams-Watts and Double Power Law functions [10] utilizing the mathematical procedure of genetic algorithm with binary representation of the theoretical attenuation function variables [13]. Using the theoretical model with Double Power Law function

$$\alpha \approx 1/\left((\omega\tau)^{-n} + (\omega\tau)^{m}\right) \tag{5}$$

the calculated lines gave an excellent agreement with the measured acoustic spectrum in the whole temperature range.

The representative acoustic spectra measured at 18 MHz of some glasses of the System I are illustrated in Fig. 2a where the change of position and proportion at the broad maxima peaks can be seen. Their theoretical simulation for two different frequencies (18 and 27 MHz) is illustrated for one sample of this set in Fig. 2b and Fig. 2c, respectively. The temperature dependencies of the acoustic attenuation were finally analyzed assuming the existence of three thermally activated relaxation processes of Cu^+ ions in connection with different kinds of sites. The proportion of the intensities of first two peaks (I_1 / I_2) depends on the glass composition, that is on the ratio CuBr/(CuI + CuBr) and reaches its maximum at x = 6.82 (BIDP3) similarly as dc conductivity. The dependences of relative intensities of individual acoustic attenuation peaks on glass composition are illustrated in Fig. 2d. The third peak, the presence of which only enables to fit the experimental dates thoroughly, represents non-essential transport mechanisms probably dependent only on glass forming system. Using the Equation (4) and values of T_{peak} for individual peaks, the activation energies E_a^a were determined (Table 1).

As it can be seen from the summarization of activation energies in Table 1, there are several categories of relaxation processes. High temperature activation energy established by all three methods, E_{a1}^{dc}, E_{a1}^a, $E_a^{tg\delta}$ presents the basic mechanism. The second mechanism observed by both acoustic and conductivity measurements E_{a2}^a, E_{a2}^{dc} can play an important roll in ionic transport, too. The existence of the processes characterized by activation energies E_{a3}^{dc}, E_{a4}^{dc} of system I is probably induced by the conditions of glass preparation and can be reduced by thermal treatment. The energy E_{a3}^a represents relaxation mechanism that does not influence the ionic transport significantly.

Comparing the activation energies obtained from acoustic and electrical measurements, it seems reasonable that essentially the same microscopic processes can be responsible for the acoustic and electrical relaxation processes. However, some differences can be caused by the different relaxation mechanisms connected with ion hopping transport at ac electric field and the hopping of mobile ions due to the interaction of acoustic wave with glass network.

The results from IR spectra of the $CuI-CuBr-Cu_2O-P_2O_5$ glasses [6-8] indicate that the thermal activated processes of Cu^+ ions determined for all samples of investigated systems can be associated

mainly with three different structural units - monomeric orthophosphate PO_4^{3-}, low-condensed dimeric diphosphate oxoanions $P_2O_7^{4-}$ and $P_3O_{10}^{5-}$ structure phosphate anions. The local electric field around the trivalent orthophosphate anion PO_4^{3-} is stronger than the local electric field around dimeric diphosphate oxoanions $P_2O_7^{4-}$ and triphosphate $P_3O_{10}^{5-}$ anions because the diphosphate and triphosphate anions has smaller negative electric charge on non-bridging oxygen atoms. Moreover expanded structure of chain groups creates advantageous conditions for ionic motion [8]. For that the electrostatic interactions between the mobile Cu^+ ions and orthophosphate anions are stronger than those between Cu^+ ions and diphosphate and triphosphate anions and we can suppose that the relaxation processes with biggest activation energies can be connected with monomeric orthophosphate anions and the processes with smaller energies can be connected with both dominant diphosphate oxoanions $P_2O_7^{4-}$ and low condensed triphosphate anions and maybe other polymeric structural units. However, the existence of two main relaxation and transport mechanisms should support the idea of two equivalent anion structural units.

Glass sample		Acoustic measurements			Electrical measurements				
Label	x [mol %]	E_{a1}^a	E_{a2}^a	E_{a3}^a	E_{a1}^{dc}	E_{a2}^{dc}	E_{a3}^{dc}	E_{a4}^{dc}	$E_a^{tg\delta}$
	y [mol %]	[eV]	[eV]	[eV]	[eV]	[eV]	[eV]	[eV]	[eV]
IDP	0	0.48	0.43	0.36	0.48	0.44	0.55	0.30	0.48
BIDP1	2.27	0.47	0.41	0.37	0.46	0.40	0.52	0.30	0.46
BIDP2	4.55	0.46	0.41	0.36	0.46	0.44	0.54	0.35	0.47
BIDP3	6.82	0.46	0.41	0.37	0.46	0.42	0.55	0.30	0.48
BIDP5	9.09	0.46	0.42	0.33	0.46	0.42	0.54	0.33	0.47
BIDP6	11.36	0.46	0.42	0.35	0.45	0.43	0.52	0.35	0.48
BIDP7	13.63	0.45	0.42	0.39	0.45	0.43	0.50	0.23	0.47
BIDP8	15.91	0.46	0.43	0.36	0.42	0.41	0.52	0.26	0.50
IPM	0	0.47	0.39	0.34	0.39	0.40	-	-	0.39
IBPM2	3.125	-	-	-	0.18	0.39	-	-	0.36
IBPM3	6.250	-	-	-	0.27	0.40	-	-	0.34
IBPM5	9.375	0.48	0.40	0.35	0.33	0.40	-	-	0.34
IBPM1	12.500	-	-	-	0.34	0.40	-	-	0.34
IBPM4	18.750	-	-	-	0.25	0.38	-	-	0.35
BPM	25.00	0.46	0.43	-	0.36	0.38	-	-	0.36

Table 1: Activation energies calculated from acoustic (E_a^a) and electric dc (E_a^{dc}) and ac ($E_a^{tg\delta}$) measurements using corresponding Arrhenius plots.

The infrared study of Cu^+ ions conducting glasses in the similar systems [6] showed that these glasses contain mainly PO_4^{3-} and MoO_4^{2-} tetrahedral anions groups and cuprous halides as well as their mixtures do not affect significantly the dominant phosphate and molybdate oxide structural units of glasses. For movement of Cu^+ ions in glass structure also the nature of anion distribution in the network is important. Structure of investigated glasses changes significantly with increasing $MoO_3/(P_2O_5+MoO_3)$ ratio [14]. With increasing content of MoO_3 in glasses increases the number of non-bridging oxygens (NBO) which is associated probably with increase in polarizability of oxygen atoms. Mixing of cuprous halides in these systems causes a negative deviation in the activation energy from the additivity rule, which corresponds with the positive deviation in electrical conductivity.

Conclusion

We have studied the correlation between the acoustic, conductivity and dielectric spectroscopy results of the set of ion conductive glasses of the systems $CuI–CuBr–Cu_2O–P_2O_5$ and $CuI-CuBr-Cu_2O-P_2O_5-MoO_3$ and several relaxation and transport mechanisms were observed. The fact that some of activation energies determined from dielectric spectroscopy and conductivity measurements on one side and acoustic attenuation spectroscopy on other side have the same or very close values ($E_{a1}{}^{a}$, $E_{a1}{}^{dc}$, $E_{a}{}^{tg\delta}$; $E_{a2}{}^{a}$, $E_{a2}{}^{dc}$) proved that the same mechanisms can influence electrical and acoustical losses in investigated ion conductive glasses.

Acknowledgements

References

[1] K. Funke, Solid State Ionics 94 (1997), p. 27

[2] R. Richter, H. Wagner, Solid State Ionics 105 (1998), p. 167

[3] M. D. Igram, Phil. Mag. 60 (1998), p. 729

[4] D. P. Almond and A.R. West, Solid State Ionics, 26 (1988), p. 265

[5] M. Cutroni, A. Mandanici, Solid State Ionics 105 (1998), p. 149

[6] M. Jamnický, P. Znášik, D. Tunega, M. D. Ingram, J.Non-Cryst.Solids 185(1995), p. 151

[7] P. Znášik, M. Jamnický, Solid State Ionics 92 (1996), p. 145

[8] P. Znášik, M. Jamnický, Solid State Ionics 95 (1997), p. 207

[9] P. Bury, P. Hockicko, M. Jamnický and I. Jamnický, in: Proc. 18th Int. Congress on Acoustics, Kyoto, 2004, Vol. II, p. 1137

[10] P. Bury, P. Hockicko, S. Jurečka, M. Jamnický, physica status solidi (c), No. 11 (2004), p. 2888

[11] P. Knauth, H. L. Tuller, J. Am. Ceram. Soc. 85 (2002), p. 1654

[12] K. Funke, B. Roling, M. Lange, Solid State Ionics 105 (1998), p. 195

[13] S. Jurečka, M. Jurečková, J. Müllerová, acta physica slovaca 53 (2003), p. 215

[14] P. Znášik, M. Jamnický, J. Non-Cryst. Solids, 146 (1992), p. 74